Perfusion-Weighted Imaging Defects During Spontaneous Migrainous Aura

F. Michael Cutrer, MD,* A. Gregory Sorensen, MD,† Robert M. Weisskoff, PhD,† Leif Østergaard, MD,† Margarita Sanchez del Rio, MD,* E. John Lee, BA,† Bruce R. Rosen, MD, PhD,† and Michael A. Moskowitz, MD*

Perfusion- and diffusion-weighted magnetic resonance imaging was performed during spontaneous visual auras in four migraineurs. Alterations in relative cerebral blood flow (16–53% decrease), cerebral blood volume (6–33% decrease), and tissue mean transit time (10–54% increase) were observed in the gray matter of occipital cortex contralateral to the affected visual hemifield. No changes in the apparent diffusion coefficient were observed either while the patients were symptomatic or after resolution of the visual symptoms but before the onset of headache. Functional magnetic resonance imaging can be a useful noninvasive tool to study hemodynamic changes during spontaneous attacks of migraine with aura.

Cutrer FM, Sorensen AG, Weisskoff RM, Østergaard L, Sanchez del Rio M, Lee EJ, Rosen BR, Moskowitz MA. Perfusion-weighted imaging defects during spontaneous migrainous aura. Ann Neurol 1998;43:25–31

Brain hemodynamics during spontaneous migraine aura and headache are incompletely understood largely because the methods for characterizing and capturing attacks have not been readily available. Most often, the attacks occur without warning and are relatively short-lived. Patients with visual symptoms induced by carotid puncture were studied with serial cerebral blood flow determinations using intracarotid xenon 133.[1] Localized decreases in occipital lobe perfusion developed, which spread anteriorly.[1] The blood flow changes, which persisted well beyond the aura and into the headache phase were moderate in magnitude.[1] and thus conflicted with widely proposed notions about the ischemic origins of the clinical manifestations. Some questioned whether relative cerebral blood flow (rCBF) changes were underestimated because of artifacts related to Compton's scatter.[2,3] Others questioned whether the blood flow changes seen during attacks might have been induced by traumatic procedures such as carotid artery puncture and catheterization.[4] A single spontaneous episode of migraine was recently captured by using positron emission tomography (PET) while the subject was being studied for other purposes. In this case decremental blood flow changes were observed, despite the fact that the expanding scotoma typical of classic migraine was not present.[5]

Although providing very useful information, neither intracarotid xenon 133– nor PET-based blood flow techniques are practical for studying spontaneous and short-lived events like the migraine aura. This report represents the first series of patients studied during typical spontaneous migraine auras. To our knowledge, it is the first series in which functional magnetic resonance imaging (fMRI) technology was applied during noninduced migraine aura.

Materials and Methods

Magnetic Resonance Imaging Methods

Data were obtained both during aura and interictally (migraine-free for at least 1 week) in all subjects using conventional, hemodynamic, and diffusion-weighted MRI techniques. All imaging was performed on a 1.5-T Signa system (General Electric, Waukesha, WI) modified for echo-planar imaging with a retrofit by Advanced NMR Systems Inc (Wilmington, MA). Conventional imaging included sagittal T1-weighted spin-echo imaging and axial T2- and proton density–weighted fast spin-echo imaging. Conventional images were acquired with standard system software.

HEMODYNAMIC IMAGING. Hemodynamic (perfusion-weighted) imaging was obtained by performing T2-weighted spin-echo, echo-planar imaging (EPI) during the injection of a high susceptibility paramagnetic contrast medium (gadodiamide, Nycomed, Inc, Princeton, NJ). In this technique, a bolus injection of the contrast medium induces a transient signal drop in the brain, reflecting an increase in the rate of T2 relaxation proportional to the concentration of the con-

From *Stroke and Neurovascular Regulation, Departments of Neurology and Neurosurgery, and †Nuclear Magnetic Resonance Center, Department of Radiology, Massachusetts General Hospital, Harvard Medical School, Charlestown, MA.

Received Apr 3, 1997, and in revised form Aug 15. Accepted for publication Aug 18, 1997.

Address correspondence to Dr Moskowitz, Massachusetts General Hospital, 149 13th St, CNY 6403, Charlestown, MA 02129.

trast media in the brain parenchyma.[6] A variety of maps can be synthesized from these concentration-versus-time data, including maps of relative cerebral blood volume (rCBV) and, more recently, rCBF.[7–12] Each of 10 slice planes was sampled once every 1.5 seconds to adequately sample the time course of the bolus passage of contrast. The 10 slices were located based on clinical examination and reported symptoms.

These images were then processed to create maps of rCBV by converting the time–intensity curve to a curve of first change in T2 rate ($\Delta R2$) proportional to the contrast agent concentration versus time. rCBV was then computed using a numerical integration technique as described previously.[13–15] Maps of rCBF were derived from estimation of peak T2 rate change after deconvolution of the tissue concentration/time curve with the arterial input function derived directly from the MR image data.[11,12,16] Mean transit time (MTT) maps are the pixelwise ratio of our CBV/CBF images. Perfusion imaging postprocessing routines include a Hanning kernel (3×3) for spatial smoothing.

DIFFUSION-WEIGHTED IMAGING. Diffusion-weighted images were acquired using a Stejskal-Tanner spin-echo EPI technique that samples the trace of the water self-diffusion tensor.[17] This technique uses single-shot imaging at both high and low b values in three orthogonal directions, from which quantitative maps of isotropic apparent diffusion coefficient (ADC) can be computed. Both trace ADC and isotropic diffusion-weighted images were available for analysis.

Data Analysis

Multislice data were collected in each session. Conventional T2-weighted images as well as postcontrast T1-weighted images were visually inspected for changes. For quantification, a region of interest (ROI) (~130 pixels each) was drawn over the gray matter of the visual cortex on a single slice based on the MRI templates of Damasio and Damasio.[18] Anatomical landmarks were used to verify that the most similar slice from each study was chosen. To adjust for minor asymmetries present interictally, results are expressed as a ratio of the affected (contralateral to visual field defect) ROI over the nonaffected ROI during aura divided by the same ratio obtained during the interictal state. Visual comparison was also made between the occipital lobes and other brain regions.

Case Histories

All subjects provided informed consent and fulfilled the International Headache Society diagnostic criteria for migraine with aura.[19] None of the subjects took acute migraine medication before scanning or were taking a prophylactic medication at the time of the studies. In addition to studies performed during visual aura, interictal perfusion and diffusion-weighted studies were performed in all subjects.

Subject 1

Three separate migraine attacks were captured in Subject 1 (two during stereotypical migraine visual aura and one during headache after a similar aura). A 38-year-old male physician (F.M.C.) with a 24-year history of recurrent migraine (one per month) noticed a small central scotoma with a scintillating temporal margin in his left visual field. Over the next 25 minutes, the image gradually expanded to involve the entire hemifield but did not cross the midline. Dynamic contrast imaging and standard T2-weighted imaging were performed 25 minutes after onset (study 1a) and were completed before the visual symptoms resolved. Within 1 hour after resolution, a moderate right-sided, throbbing headache developed associated with mild nausea and photophobia lasting for 12 hours.

Ten months after study 1, another stereotypical migrainous episode developed, which was studied using dynamic contrast imaging and diffusion-weighted imaging (study 1b) 35 minutes into the aura. A second perfusion- and diffusion-weighted scan was obtained after the resolution of the visual symptoms but before the headache during the same attack (study 1c).

Perfusion-weighted imaging (study 1d) was also performed 2.5 hours after resolution of stereotypical visual symptoms during a moderate right frontal headache with nausea and photophobia.

Subject 2

A 64-year-old male physicist with a history of recurrent migraine extending back to childhood experienced the onset of a visual disturbance that consisted of "zigzag lines" in the left hemifield of vision. Dynamic contrast imaging and diffusion-weighted imaging were performed while his vision was obscured (study 2). By the end of the standard T2-weighted scan, he reported resolution of the visual disturbance. He has a strong family history of migraine and has experienced attacks both with and without visual aura. His headaches occur several times per month, and severe attacks are characterized by unilateral throbbing pain and occasional nausea. He has no history of stroke.

Subject 3

A 36-year-old male hospital administrator with a 10-year history of severe recurrent throbbing headaches associated with mild nausea and intense photo/phonophobia noticed the onset of a familiar visual disturbance that he described as "dancing light." His headaches occurred about once per week, and in the past, similar visual symptoms preceded many but not all of his headache attacks. The visual hallucination gradually expanded in an "amebic" manner to obscure a large part of his left visual field. Twenty minutes after the onset of dancing lights, he underwent dynamic contrast and then diffusion-weighted imaging (study 3a). Twenty-five minutes later, the diffusion-weighted imaging was repeated after resolution of the visual symptoms and just before the onset of a moderate right-side throbbing headache (study 3b).

Subject 4

A 43-year-old female physician with a 20-year history of recurrent headaches associated with nausea and photophobia and preceded by visual disturbance noted the appearance of "muted colors of flashing or vibrating light" in the right visual hemifield. With this attack, the visual disturbance, although present in both eyes, appeared more prominent in the right eye and gradually resolved as the disturbance spread peripherally. Perfusion-weighted imaging was begun during

the last minutes of visual symptoms and before the onset of headache (study 4). The subject had a family history of recurrent migraine and suffered from typical attacks every few months.

Results

Anatomical T2-weighted images obtained ictally and interictally were normal in all subjects.

Perfusion-Weighed Imaging

Interictally, rCBF, rCBV, and MTT were normal and symmetrical throughout the cerebrum in all 4 subjects. Within the occipital lobes, the interictal ratios for rCBF, rCBV, and MTT within the subsequently affected ROI/unaffected ROI were 106.0 ± 2% (mean ± SEM), 103.9 ± 2%, 102.3 ± 5%, respectively.

During visual aura, changes in rCBF, rCBV, and MTT were qualitatively similar in all subjects and differed only in magnitude (Table). Within the ROI on the affected side (1) decreases in rCBF ranging from 16 to 53% were observed, (2) rCBV was decreased (range, 6–33%) although to a lesser extent than rCBF, and (3) MTT was increased by 10 to 36%. Other regions of the brain (eg, frontal lobes and contralateral occipital lobe) remained without change.

A more detailed evaluation of migraine-related hemodynamic change was performed in Subject 1. Perfusion-weighted imaging was obtained interictally and during three separate stereotypic attacks at four different time points (Fig 1). When no aura was present the ratio of the rCBF in the right hemisphere to the rCBF in the left hemisphere was 1.09 (Fig 2). When imaged at 25 minutes after the onset of symptoms (study 1a), this ratio dropped by 37% to 0.68. During the second study at 35 minutes after onset (study 1b), the findings on the initial perfusion-weighted imaging were consistent with study 1, again with no change in the left occipital lobe.

Visual inspection suggested an anterior extension of the rCBF and MTT abnormalities between the 35- (1b) and 59-minute (1c) time points. Consistent with this observation, the blood flow within an ROI just anterior to the perfusion abnormality on the affected side was 14% lower than blood flow in the corresponding ROI on the contralateral (nonaffected) side. At 59 minutes, the blood flow within this same ROI was 29% lower compared with the ROI on the contralateral side (see Fig 1 rCBF for ROI used).

In study 1d, 2.5 hours after resolution of symptoms, less severe hypoperfusion persisted in the same location. There was no evidence of hyperemia (the CBV measured 19% below baseline).

Diffusion-Weighted Imaging

In all subjects in whom diffusion-weighted images were obtained during visual symptoms, there was no evidence of regional hyperintensity to suggest decreases in water mobility (Fig 3). Quantitative maps of ADC were symmetrical and normal in all the available subjects during both the aural and the postaural scans (see Table). The range of variation of the technique is estimated by us (A.G.S.) to be 8 to 10%.

Table. Subjects Imaged During Migraine Visual Aura

Study No.	Age (yr)	Aura Abnormal Visual Field	Time from Onset of Aura to MRI	rCBF Findings	rCBV Findings	MTT	DWI Findings
1	38	1a. L visual hemifield	25 min	37% decrease, R occipital lobe	16% decrease	31% increase	Not available
		1b. L visual hemifield	35 min	53% decrease, R occipital lobe	33% decrease	36% increase	5% increase in ADC
2	64	2. L visual hemifield	30 min	21% decrease, R occipital lobe	19% decrease	10% increase	4% increase in ADC
3	36	3. L visual hemifield	20 min	35% decrease, R occipital lobe	17% decrease	25% increase	6% decrease in ADC
			45 min				3% decrease in ADC
4	43	4. R visual hemifield	35 min	16% decrease, L occipital lobe	6% decrease	11% increase	Not available

Perfusion- and diffusion-weighted imaging in gray matter of occipital lobe contralateral to visual field defect.

MRI = magnetic resonance imaging; rCBF = relative cerebral blood flow; rCBV = relative cerebral blood volume; MTT = mean transit time; DWI = diffusion-weighted imaging; L = left; R = right; ADC = apparent diffusion coefficient.

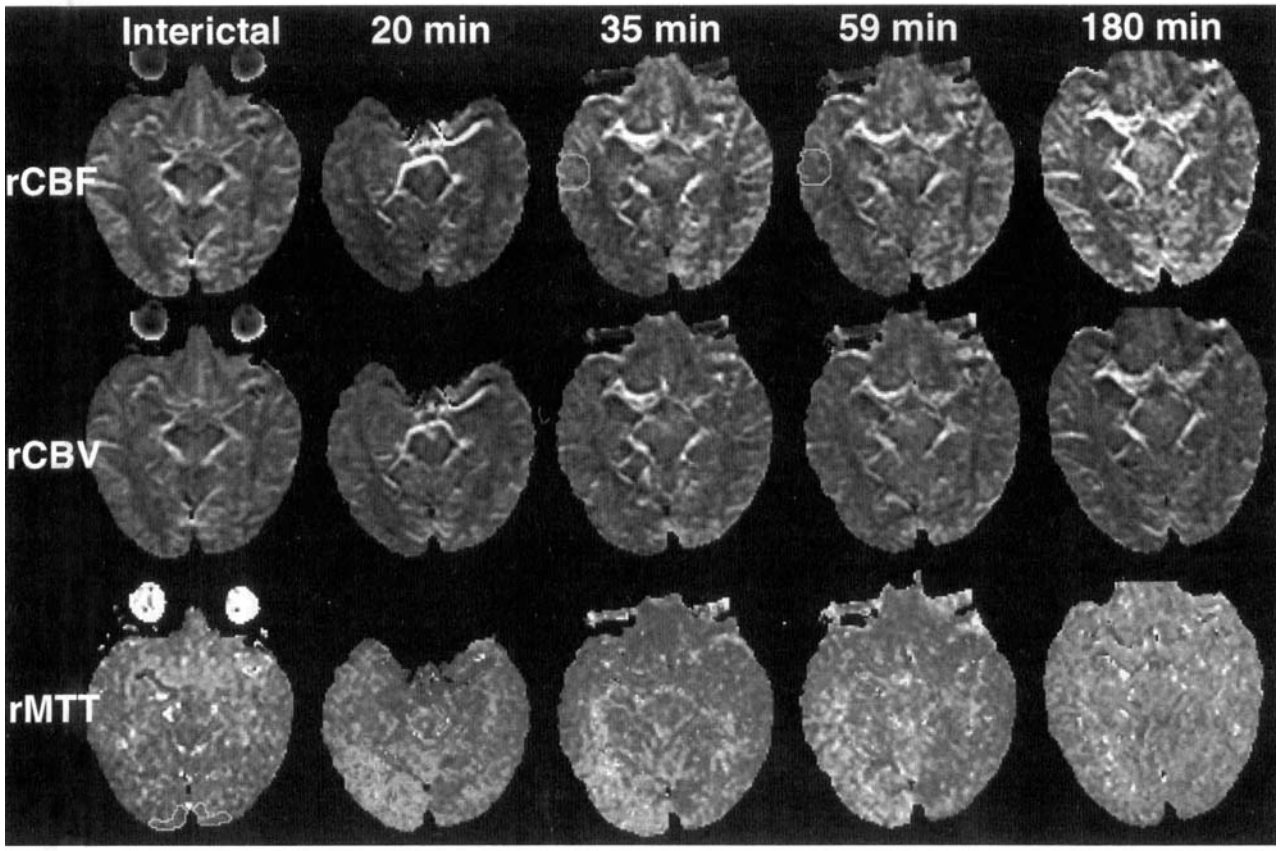

Fig 1. Hemodynamic images during left visual field disturbance show decreased flow and volume in the right occipital lobe, with increased mean transit time. Perfusion-weighted images obtained interictally and at four time points (20, 35, 59, and 180 minutes) after onset of visual aura affecting the left visual field. At the 20- and 35-minute time points, visual symptoms were present. At 59 minutes, visual symptoms had resolved but headache had not begun. At 180 minutes, moderate right-sided headache and mild nausea were present. rCBF = relative cerebral blood flow; rCBV = relative cerebral blood volume; MTT = mean transit time. The region of interest (ROI) superimposed on the interictal time point of MTT represents the ROI used in the quantitative analysis in all parameters at all time points during the analysis. The ROIs superimposed on the rCBF map at 35 and 59 minutes illustrate that decremental change along the anterior margin of the perfusion defect increased with time. Parameters for hemodynamic weighted imaging are as follows: imaging plane: axial; field of view (cm), 20 × 40; resolution (pixels), 128 × 256 (= 1.56 × 1.56 mm pixels); repetition time (msec), 1,500; echo time (msec), 72; slice thickness (mm), 6; interslice gap, 1 mm; number of slices, 10; number of averages, 1; images per slice, 51; total number of images, 510; total imaging time, 83 seconds. The contrast agent injection is performed at 5 ml/sec, using an MR-compatible power injector (Medrad, Pittsburgh, PA) 10 seconds after the start of imaging. Gadolinium dose, 0.15 mmol/kg.

Discussion

Using fMRI technology, we observed moderate focal reductions in cerebral blood flow and volume in the occipital lobe during multiple spontaneous migraine visual auras in 4 subjects. The occipital lobe perfusion deficits corresponded neuroanatomically with the reported visual field disturbance and with the side of the subsequent headache. Reductions in blood flow decreased in magnitude after resolution of visual symptoms. The variability of estimated reductions in rCBF, which ranged from 16 to 53%, may be explained by interindividual variation or by differences in the time at which imaging was performed. Smaller decreases in rCBF were seen in Patients 2 and 4 in whom imaging was performed toward the end of the aura symptoms.

The moderate reductions in rCBF that we observed are consistent with prior published studies.[1,20–23] using xenon 133 blood flow techniques. We conclude that the methods previously used to induce a migraine attack, such as carotid puncture, did not cause the measured hemodynamic changes during aura and headache directly and that the hemodynamic findings previously reported appear to mimic closely those observed during spontaneous aura. Our findings are also consistent with blood flow data obtained during a spontaneous migraine headache with an atypical visual disturbance,[5] using PET and oxygen 15–labeled water.

The symptoms of migraine aura have traditionally

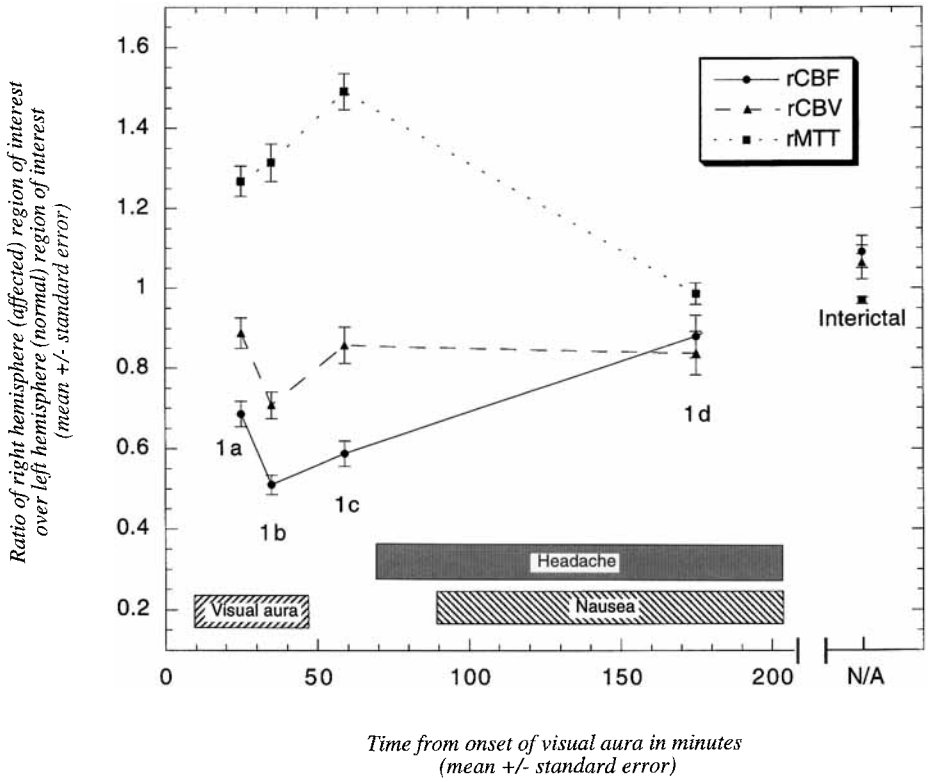

Fig 2. Gray matter hemodynamic changes in migraine visual area as measured with magnetic resonance imaging—temporal course of hemodynamic and diffusion measurements. The y *axis represents the measurement made in the right (affected) occipital lobe region of interest (ROI) divided by the measurement made in the left occipital lobe ROI. ROI is shown in the interictal rMTT of Figure 1. Symptoms are indicated by the bars. Data points were obtained from four different studies and demonstrate the decrease and subsequent resolution over time of blood flow to the right (affected) occipital lobe. Error bars represent SEM of the approximately 130 pixels within each ROI. rCBF = relative cerebral blood flow; rCBV = relative cerebral blood volume; rMTT = relative mean transit time.*

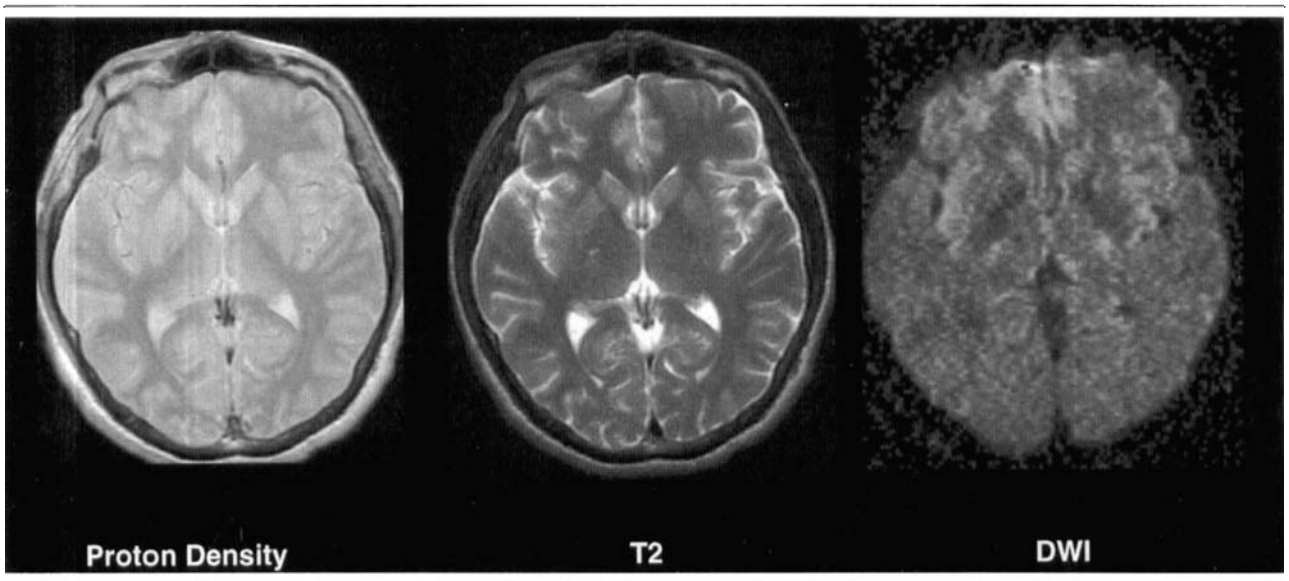

Fig 3. Ictal diffusion-weighted imaging (DWI) and conventional imaging are normal. Proton density image, conventional T2-weighted fast spin-echo image, and DWI with a b *value of 1,009 sec/mm^2 are shown. Parameters for DWI: imaging plane: axial; field of view (cm) 20 × 40; resolution (pixels), 128 × 256 (= 1.56 × 1.56 mm pixels); number of slices, 17; repetition time (msec), 6,000; echo time (msec), 151;* b *values: 1,009, 47 sec/mm^2; number of averages, 3; total acquisition time, 132 seconds.*

been explained on an ischemic basis. Although the moderate rCBF reductions (mean, 32.4 ± 7%) we observed suggest that severe ischemia was probably not responsible for the symptoms during the visual auras we studied, based on these preliminary data from perfusion-weighted imaging, we cannot exclude some period of shortfall between energy supply and demand.

We observed no significant change in water diffusion during or after spontaneous migraine aura despite drops in rCBF of up to 53%. These data may shed

light on two proposed mechanisms for migraine aura, ischemia and spreading depression.[24] With regard to ischemia, infarcts are seen only rarely after aura. However, the aura-associated hypoperfusion seen in our and others' data might still be the cause of the neuronal dysfunction due to transient ischemia. What does normal diffusion imaging tell us about this possibility? We know from our clinical observations that once tissue becomes abnormal on diffusion-weighted imaging, infarction is virtually certain, with fewer than 1 of 1,000 cases showing spontaneous regression.[25] We also know that some tissue can be normal on hyperacute diffusion studies despite hypoperfusion; these areas of "mismatch" between diffusion-weighted imaging and hemodynamic-weighted MRI often go on to infarct, indicating that diffusion-weighted imaging abnormalities take some time to develop even with severe hypoperfusion. The precise meaning of diffusion abnormalities (or lack thereof) in the evolution of ischemic damage in humans remains to be clarified. Nevertheless, based on our experience in human stroke, we know that measurable diffusion abnormalities indicate that a metabolic threshold has been crossed in the cascade of ischemic damage, possibly irreversibly. The absence of such abnormalities in our migraine aura data indicates that this threshold is not crossed during the aura. This does not exclude ischemia, but it indicates that if ischemia is present, it is not severe or persistent enough to cause whatever changes ADC abnormalities represent.

Diffusion imaging has also been used in animal models to visualize changes associated with spreading cortical depression (SD),[26,27] although no human SD visualization with MRI has been reported. We also do not see MRI changes corresponding to SD in our aura patients, despite a "spreading" of the perfusion defect in one of our subjects and despite ongoing neurological defects. This might be because SD is not present at a level detectable by our methodology, or perhaps it is not present at all. We are currently developing more sensitive techniques to detect SD and continue to search for this phenomenon in migraine aura and a variety of other neurological diseases.

Hyperemia, as measured by single-photon emission computed tomographic and xenon blood flow methods,[23] has sometimes developed during headache but often not until hours after onset. We found no evidence for cerebral blood flow or blood volume increases at any measured time point in our patients. Perfusion imaging can detect flow and volume changes in cortical and leptomeningeal vessels, although it may not detect such changes in dural vessels.[28] Hence, dilation of small cortical vessels does not appear to be necessary for the generation of headache. These preliminary findings agree with those in the literature, ie, that blood volume and flow do not correlate well with the presence of headache.

The use of fMRI to study migraine offers several distinct advantages over the use of other functional imaging techniques. fMRI is noninvasive, requires no radioactivity, and can potentially measure multiple parameters including oxygen hemoglobin saturation and transmembrane water mobility as well as rCBF and rCBV. Repeated sequential images during the time constraints of the migraine aura are possible. The resolution of fMRI is better than that using xenon blood flow techniques and at least as good as PET. Repeated study of juxtaposed neuronal and vascular functional parameters within a single short-lived neurological event likely presents a unique opportunity to define changes in brain metabolism and flow accompanying migraine aura.

This study was supported in part by National Public Health Service grants R01-CA40303, P01-CA48729 (B.R.R.), K08 NS 01803 (F.M.C.), and NS 35611 (M.A.M.), a Scholar Grant from the Radiological Society of North America (A.G.S.), an IHS 1997 Research Fellowship award (M.S.d.R.), a Glaxo Pharmaceuticals small grants award, and an Unrestricted Award for Research in Neuroscience from Bristol-Myers Squibb.

We thank Terrence Campbell and Mary Foley for their technical assistance.

References

1. Olesen J, Larsen B, Lauritzen M. Focal hyperemia followed by spreading oligemia and impaired activation of rCBF in classic migraine. Ann Neurol 1981;9:344–352
2. Olsen TS, Friberg L, Lassen NA. Ischemia may be the primary cause of the neurologic deficits in classic migraine. Arch Neurol 1987;44:156–161
3. Olsen TS. Spreading oligemia in the migraine aura—most likely an artifact due to scattered radiation. Cephalalgia 1993; 13:86–88
4. Raskin NH. Headache. 2nd ed. New York: Churchill Livingstone, 1988:101–103
5. Woods RP, Iacoboni M, Mazziotta JC. Brief report: bilateral spreading cerebral hypoperfusion during spontaneous migraine headache. N Engl J Med 1994;331:1689–1692
6. Villringer A, Rosen BR, Belliveau JW, et al. Dynamic imaging with lanthanide chelates in normal brain: contrast due to magnetic susceptibility effects. Magn Reson Med 1988;6:164–174
7. Rosen B, Belliveau J, Vevea J, Brady T. Perfusion imaging with NMR contrast agents. Magn Reson Med 1990;14:249–266
8. Rosen BR, Belliveau JW, Aronen HJ, et al. Susceptibility contrast imaging of cerebral blood volume: human experience. Magn Reson Med 1991;22:293–299
9. Rosen B, Belliveau J, Buchbinder B, et al. Contrast agents and cerebral hemodynamics. Magn Reson Med 1991;19:285–292
10. Rosen BR, Aronen HJ, Kwong KK, et al. Advances in clinical neuroimaging: functional MR imaging techniques. Radiographics 1993;13:889–896
11. Østergaard L, Weisskoff R, Chesler D, Gyldensted C, et al. High resolution measurement of cerebral plasma flow using intravascular tracer bolus passages. Part I: Mathematical approach and statistical analysis. Magn Reson Med 1996;36:715–725
12. Østergaard L, Sorensen AG, Kwong K, et al. High resolution

measurement of cerebral blood flow using intravascular tracer bolus passages. Part II: Experimental Comparison and Preliminary Results. Magn Reson Med 1996;36:726–73
13. Aronen H, Gazit I, Louis D, et al. Cerebral blood volume maps of gliomas: comparison with tumor grade and histologic findings. Radiology 1994;191:41–51
14. Boxerman J, Weisskoff R, Aronen H, et al. Signal-to-noise and tissue blood volume maps from dynamic NMR imaging studies. Society of Magnetic Resonance in Medicine 11th Annual Meeting, Berlin, 1992:1130 (Abstract)
15. Weisskoff R, Boxerman J, Sorensen A, et al. Simultaneous blood volume and permeability mapping using a single Gd-based contrast injection. Proceedings of the Second Meeting of the Society of Magnetic Resonance, San Francisco, 1994:279
16. Porkka L, Neuder M, Hunter G, et al. Arterial-input function measurement with MRI. Society of Magnetic Resonance in Medicine 10th Annual Meeting, San Francisco, 1991:120 (Abstract)
17. Sorensen A, Weisskoff R, Reese T, et al. Optimization of diffusion-weighted MR imaging for evaluation of acute stroke. Proceedings of the Third Meeting of the Society of Magnetic Resonance, Nice, France, 1995:1383
18. Damasio H, Damasio AR. Lesion analysis in neuropsychology. New York: Oxford University Press, 1989:184–187
19. Headache Classification Committee of the International Headache Society. Classification and diagnostic criteria for headache disorders, cranial neuralgias and facial pain. Cephalalgia 1988; 8(Suppl 7):1–96
20. Olesen J, Friberg L, Olsen TS, et al. Timing and topography of cerebral blood flow, aura and headache during migraine attacks. Ann Neurol 1990;28:791–798
21. Lauritzen M, Skyhoj Olsen T, Lassen NA, et al. Changes of regional cerebral blood flow during the course of classical migraine attacks. Ann Neurol 1983;13:633–641
22. Lauritzen M, Olesen J. Regional cerebral blood flow during migraine attacks by xenon-133 inhalation and emission tomography. Brain 1984;107:447–461
23. Andersen AR, Friberg L, Olsen TS, et al. SPECT demonstration of delayed hyperemia following hypoperfusion in classic migraine. Arch Neurol 1988;45:154–159
24. Milner PM. Note on a possible correspondence between the scotomas of migraine and spreading depression of Leao. EEG Clin Neurophysiol 1958;10:705
25. Sorensen A, Buonanno F, Gonzalez R, et al. Evaluation of hyperacute stroke using multislice echo planar diffusion-weighted and hemodynamic MR imaging. Radiology 1996;199:391–401
26. Haseqawa Y, Latour LL, Formato JE, et al. Spreading waves of a reduced diffusion coefficient of water in normal and ischemic rat brain. J Cereb Blood Flow Metab 1995;15:179–187
27. Gardner-Medwin AR, van Bruggen N, Williams SR, et al. Magnetic resonance imaging of propagating waves of spreading depression in the anaesthetised rat. J Cereb Blood Flow Metab 1994;14:7–11
28. Weisskoff R, Zuo C, Boxerman J, et al. Microscopic susceptibility variation and transverse relaxation: theory and experiment. Magn Reson Med 1994;31:610–614